

A Survey of Recent Applications of the PISALE Code and PDE Framework

Alice Koniges

Information and Computer Sciences
University of Hawai'i at Mānoa
 Honolulu, HI, USA
 email: koniges@hawaii.edu

David Eder

Physics and Astronomy
University of Hawai'i at Mānoa
 Honolulu, HI, USA
 email: dceder@hawaii.edu

Jonghyun Lee

Civil & Env Eng and Water Res Center
University of Hawai'i at Mānoa
 Honolulu, HI, USA
 email: jonghyun.harry.lee@hawaii.edu

Aaron Fisher

Information Technology Services
University of Hawai'i at Mānoa
 Honolulu, HI, USA
 email: fallen@andcheese.org

Yuriy Mileyko

Mathematics
University of Hawai'i at Mānoa
 Honolulu, HI, USA
 email: ymileyko@hawaii.edu

Monique Chyba

Mathematics
University of Hawai'i at Mānoa
 Honolulu, HI, USA
 email: chyba@hawaii.edu

Jack McKee

Mathematics
University of Hawai'i at Mānoa
 Honolulu, HI, USA
 email: jmckee@math.hawaii.edu

Young-Ho Seo

Civil & Env Eng and Water Res Center
University of Hawai'i at Mānoa
 Honolulu, HI, USA
 email: yhseo@hawaii.edu

Peter Yip

Aerospace Engineering and Mechanics
University of Minnesota
 Minneapolis, MN, USA
 email: yipxx043@umn.edu

Thomas Schwartzenuber

Aerospace Engineering and Mechanics
University of Minnesota
 Minneapolis, MN, USA
 email: schwart@umn.edu

Claudia Parisuaña

Department of Mechanical Engineering
Stanford University
 Stanford, CA USA
 email: cparisua@stanford.edu

Siegfried Glenzer

SLAC National Accelerator Laboratory
Stanford University
 Menlo Park, CA USA
 email: glenzer@slac.stanford.edu

Abstract—We review the basic equations, numerical solution techniques, and new application areas of a novel multi-purpose computer code framework, PISALE, for the solution of complex Partial Differential Equation (PDE) systems on modern computing platforms. We describe how the code solves equations in the fluid approximation using a novel combination of Arbitrary Lagrangian Eulerian (ALE) and Adaptive Mesh Refinement (AMR) methods. Sample problems from areas of ground water flow, high-speed impacts, and X-ray Free Electron Laser (XFEL) experiments are given.

Keywords—*Adaptive Mesh Refinement; Computational Fluid Dynamics; Arbitrary Lagrangian Eulerian Methods; Volume of Fluid; High Performance Computing; Surface Tension; Ground Water Flow.*

I. INTRODUCTION

The PISALE codebase contains a Partial Differential Equation (PDE) solver framework based on the combined methods of Arbitrary Lagrangian Eulerian (ALE) dynamics and structured Adaptive Mesh Refinement (AMR). The PISALE code uses an explicit time-marching Lagrange step to advance the flow-field through a physical time step. The optional second phase involves a modification of the grid and a remapping (interpolation) of the solution to the new grid. The solution of PDEs on modern High Performance Computing (HPC) platforms is essential to the continued success of research

and modeling for a wide variety of areas. The PISALE code name comes from the acronym Pacific Island Structured-AMR with ALE. In some earlier papers (e.g., [10]) the code is called ALE-AMR as it was one of the first codes to combine those two methods. There are several branches of PISALE to deal with disparate applications. These applications range from high energy density physics problems to geothermal flows. In this paper, we detail some of the wide variety of applications suitable for modeling with PISALE and discuss recent improvements to the code base.

In Section II, we give an overview of the equations used in the PISALE code. In Subsection II-A, we describe how the different physics modules are coupled using operator splitting. We also provide some additional information on the surface tension modules used in PISALE. In Section III, we give a summary of past PISALE applications followed by discussion on modeling groundwater flow in Subsection III-A. We then discuss recent hypervelocity impacts simulations with a comparison of PISALE results with experimental data and with results from other codes in Subsection III-B. The third new application is discussed in Subsection III-C, where we describe the modeling of droplet dynamics. We provide some conclusions and comments on future work in Section IV.

II. PISALE EQUATIONS

The numerical methodology of PISALE was initially developed for pure gas dynamics and its novelty at the time was based on the coupling of AMR with a Lagrangian formulation that retains accuracy in standard two- and three-dimension problems, such as Sedov blast wave simulations [1]. By adding a complex Right Hand Side (RHS) to the basic gas dynamics with elastic/plastic flow terms, we are able to use operator splitting methods to model an extremely diverse variety of physical processes, each affecting the dynamically evolving fields at successive time intervals according to timescales. An example of a complex RHS is the use of anisotropic material failure models with material history in multi-material problems. Unlike the first implementations of these numerical techniques such as Wilkins [26], PISALE was written from the ground-up to be modular and take advantage of parallelism opportunities on HPC platforms. PISALE operates on top of the Structured AMR Application Interface (SAMRAI) library [8] and contains a general purpose PDE solver that uses a staggered-grid, Lagrangian formulation, written for coupled plasma/fluids with position and velocity being nodal variables and density, internal energy, temperature, pressure, strain, and stress being zonal (cell centered) variables. This basic solver is primarily for equations that can be written in conservation form and uses a volume of fluid approach. Thermal conduction and radiation transport coupled to the basic conservation law equations are solved by implementing the diffusion approximation, which uses a nodal radiation energy and a zone-averaged nodal temperature. These plasma/fluid equations in a Lagrangian formulation (in vector and indicial notation $i, j, k = 1, 2, 3$) are:

$$\frac{D\rho}{Dt} = -\rho\nabla \cdot \vec{U} = \rho U_{i,i} \quad (1)$$

$$\frac{D\vec{U}}{Dt} = \frac{1}{\rho}\nabla \cdot \boldsymbol{\sigma} = \frac{1}{\rho}\sigma_{ij,j} \quad (2)$$

$$\frac{De}{Dt} = \frac{1}{\rho}V\boldsymbol{s} : \dot{\boldsymbol{\epsilon}} - P\dot{V} = \frac{1}{\rho}V(s_{ij}\dot{\epsilon}_{ij}) - P\dot{V} \quad (3)$$

where $\frac{D}{Dt} = \frac{\partial}{\partial t} + \vec{U} \cdot \nabla$ is the substantial derivative, ρ is the density, $\vec{U} = (u, v, w)$ is the material velocity, t is time, $\boldsymbol{\sigma}$ is the total stress tensor, P is the pressure, e is the internal energy, V is the relative volume ($\rho V = \rho_0$ where ρ_0 is the reference density), \boldsymbol{s} is the deviatoric stress defined as $s_{ij} = \sigma_{ij} + P\delta_{ij}$ where δ is the Kronecker delta and $\dot{\boldsymbol{\epsilon}}$ is the strain rate tensor. PISALE has a range of different strength and failure models that can be used for impact and other applications.

A. PISALE Physics Modules

PISALE has significant physical modeling capabilities in addition to the core ALE hydrodynamics and structural mechanics. These capabilities are provided through a flexible physics module system which allows their PDEs to be updated separately from the hydrodynamic models with a classical operator splitting scheme. Field variables in these physics modules are advanced in time after the hydrodynamic time

step and the modules have hooks that allow them to update the field quantities when the ALE hydrodynamics alters the underlying mesh. Physical models provided in this manner include a laser ray tracing package [14], various surface tension models [11] [12], heat conduction, and diffusion-based radiation transport [7].

PISALE includes infrastructure to lower the barriers for the introduction of additional physics modules. Currently, this includes tools for transforming data and meshes from a block structured format to an unstructured indexing format, tools for tracing rays through meshes, and a basic Finite Element Method (FEM) framework for discretizing PDEs, see Figure 1. Field data in PISALE physics modules is updated after the ALE hydrodynamics step is complete. First field data is collected from the SAMRAI patch-AMR hierarchy into a parallel composite mesh, which can be utilized with unstructured solvers. Then FEM-based PDE discretizations are applied on the composite mesh to update the relevant field data. The updated field data on the composite mesh is then transformed back into the patch-AMR hierarchy. This approach enables the development of external solvers for PISALE without requiring the data to be represented as a SAMRAI patch hierarchy.

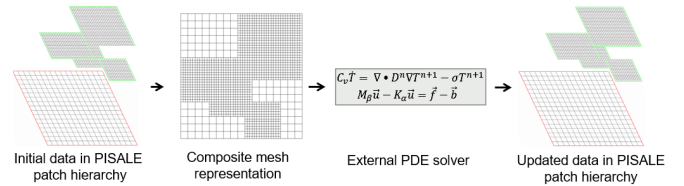


Fig. 1. Field data on PISALE patch mesh is transferred to composite mesh prior to solution by external PDE solver and then updated on patch mesh.

The current PISALE FEM framework includes only first order H^1 quadrilateral and hexahedron elements in 2D and 3D. This works well for the diffusion equation solvers utilized in the heat conduction and radiation diffusion modules. We are exploring the addition of elements from the $H(curl)$, $H(div)$, and L^2 spaces that would open up a path to discretizing a wider array of PDEs in topic as diverse as: plasma physics, mesoscale material modeling, seismicity in geophysics, and electromagnetics. The current FEM framework in PISALE only supports AMR in 2D. We are exploring FEM frameworks with 3D AMR capability that would improve the existing heat conduction, radiation diffusion, and surface tension models in PISALE. Some examples are Modular Finite Element Methods (MFEM) library [16] and the Multiphysics Object-Oriented Simulation Environment (MOOSE) [17].

1) *Surface Tension*: A major use case of the operator splitting system is the surface tension package, which models 2D and 3D surface tension using a multi-fluid Volume-of-Fluid (VOF) paradigm[4]. The VOF paradigm avoids tracking an explicit representation of fluid boundaries, instead reconstructing them at each time step based on the relative volume fractions of each fluid within every cell. This was chosen because volume fractions are already a core aspect of PISALE's multi-material formulation, meaning the surface tension package

only needs to generate and apply a body force. A height function for each fluid is generated by summing up relative volume fractions along columns of a 3x5 or 3x3x5 stencil. Orientation and position of the stencil is chosen so that the interface is always in the central cell of the stencil, the fluid body is always on the "bottom" of the stencil, and the first derivatives of the height function are minimized. See Figure 2.

In 2D, three points are chosen based on the height function and mapped back to real coordinates, where they are used to generate a three-point circular fit of the boundary, which approximates an osculating circle. This scheme is robust to nonlinear meshes with regular column widths, but a correction term must be applied in the case of irregular column widths[15]. A circular fit of this kind can be shown second-order accurate when the mesh is regular enough[3], although is only first-order accurate when the mesh is non-orthogonal or nonlinear. Because the calculation of surface tension does not rely on mesh regularity, surface tension can be incorporated as a body force during Lagrangian time steps, allowing full ALE simulations with properly coupled surface tension effects.

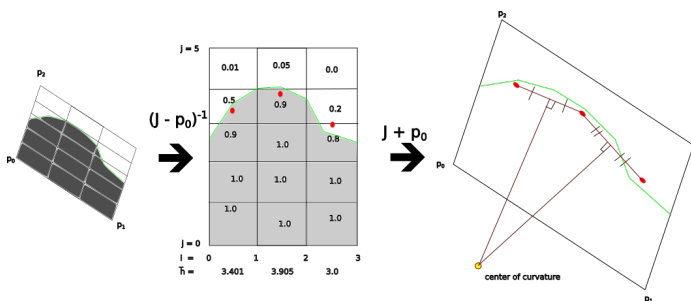


Fig. 2. Visual depiction of surface tension calculation using height functions in 2D.

In 3D, six points are chosen for a linear least-squares polynomial fit of the boundary with a quadratic polynomial $P(i, j)$ of the logical coordinates[12]. The polynomial's derivatives are then mapped through the mesh Jacobian to find first and second derivatives of the corresponding approximate parameterization $p(x, y)$ in real coordinates, which are used to calculate the mean curvature of the surface. Since the current 3D curvature calculation relies on a linear approximation of the mesh, the surface tension force can only be applied after the remap phase, and with mesh adaptation disabled.

III. RECENT APPLICATIONS AREAS

PISALE has been applied to a wide range of applications. One early application was the protection of optics and diagnostics at the National Ignition Facility (NIF) and other large laser facilities [6]. It was also used to model ion heating experiments at Neutralized Drift Compression Experiment-II (NDCX-II) to study Warm Dense Matter (WDM) properties [2]. One of the early applications that used the surface tension capability of the code was modeling the dynamics of tin droplets for extreme ultraviolet (EUV) lithography [22]. Our recent applications include groundwater flow simulations for Hawaiian

aquifers[23], impacts of particulates and rain droplets on hypersonic vehicles[27], and a range of experiments at Stanford Linear Accelerator Center (SLAC), a Department of Energy (DOE) Office of Science User Facility. Experiments include X-ray Free Electron Laser (XFEL) beam heating of hydrogen and water droplets[18] and interaction of laser produced proton beams with different materials. We summarize recent work in these three new application areas.

A. Groundwater Flow and Transport in Pacific Islands

Density-dependent miscible seawater-freshwater systems in island aquifers have been previously modeled with finite element or finite volume methods in an Eulerian framework. These simulations however, are deemed inadequate due to inappropriate grids and problems with scalability. Due to the density dependency, the governing Darcy-type flow equation is nonlinearly coupled with the mass and/or heat transport equations with a constitutive relationship, $\rho = \rho(p, T, c)$ where ρ is the density, p is the pressure, T is the temperature, and c is the salinity.

For seawater-freshwater simulation in the subsurface, the isothermal assumption, e.g., $\rho = \rho(c)$ under Boussinesq approximation is typically used for coupled flow and transport with appropriate boundary conditions [5]:

$$\nabla \cdot \mathbf{q} = 0 \quad (4)$$

$$\mathbf{q} = -\frac{\rho_0 g \mathbf{k}}{\mu} \left(\frac{\nabla p}{\rho_0 g} + \frac{\rho - \rho_0}{\rho_0} \nabla z \right) \quad (5)$$

$$\phi \frac{\partial c}{\partial t} + \nabla \cdot (\mathbf{q}c - \phi \mathbf{D}_{\text{eff}} \nabla c) = 0 \quad (6)$$

where \mathbf{q} is the fluid flux, ρ_0 is the density at the reference c and T , g is the gravity constant, \mathbf{k} is the permeability tensor of the porous medium, μ is the dynamic viscosity, ϕ is the porosity, and \mathbf{D}_{eff} is the dispersion coefficient tensor.

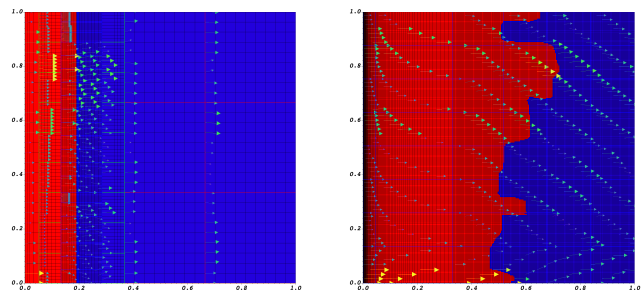


Fig. 3. Conservative tracer transport with heterogeneous hydraulic conductivity field at $t = 0$ yr (left) and 37.8 yrs (right).

A critical previously unaddressed challenge is the simulation of salinity transport in a large-scale aquifer with a spatially heterogeneous permeability field. Typically, and unsatisfactorily, coarse meshes with large diffusion coefficients (i.e., dispersivities) are implemented as numerical compromises at the cost of overestimated mixing physics. The simulated groundwater flow velocities are then used for reactive transport

modeling, which often leads to the underestimated residence time of contaminant plumes and associated overly promising groundwater remediation decisions with increasing risks of cleanup operation failure. The flexibility of PISALE, with its ability to define interfaces and the use of AMR to dynamically define the grid, addresses these issues as shown in Figure 3. We show convective tracer transport with a heterogeneous hydraulic conductivity field and its corresponding groundwater velocity. Additionally, PISALE generally reduces simulation time to a tractable problem via the parallel HPC performance of the underlying scalable SAMRAI library.

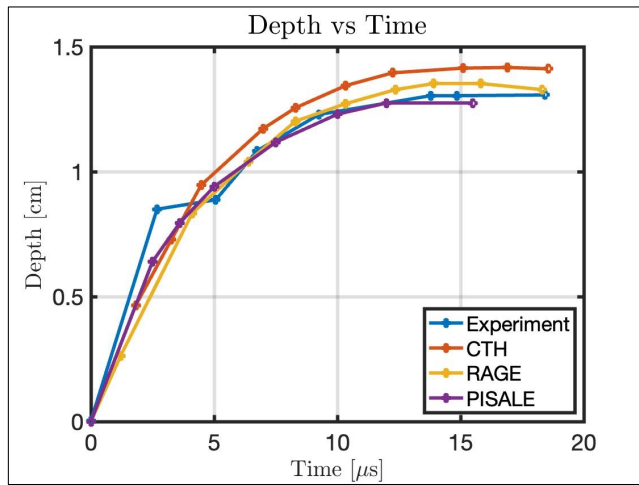


Fig. 4. Recent comparison of PISALE results with two openly published results from large code efforts (neither is open source) and experimental impact data.

B. Hypervelocity impacts

Impacts by particulates and rain droplets on hypersonic (Mach 5 and above) vehicles pose a major concern for safety of flight. It is understood that particulates of even micron-size are capable of impacting the surface quality of the vehicle [9]. Therefore, larger particles are likely to induce more surface damage and additional material erosion. To make the result more complex, the particles must traverse a shock discontinuity formed from hypersonic flight. As a particle traverses the shock, the post-shock conditions may result in a pressure, density, and temperature differential that leads to a spatio-temporal dependent particle shape change prior to making contact with the surface. PISALE offers the capability to capture such high-rate loading in a computationally cost effective manner with the implementation of AMR. PISALE has been verified and validated in its ability to capture hypervelocity impact phenomena of well-characterized ductile metals. Figure 4 shows impact crater depth in Al 6061-T6 as a function of time caused by an aluminum projectile with PISALE results in excellent agreement with experimental data [20]. The projectile has a diameter of $6.35mm$ and a velocity of $7 km/s$. Figure 5 shows the PISALE simulation of the impact at three times.

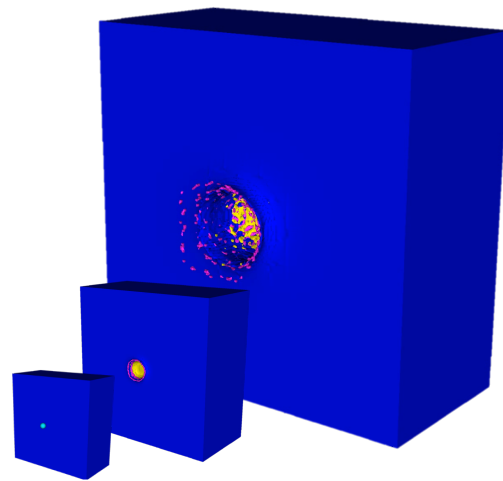


Fig. 5. PISALE simulation showing time of impact and crater at 5 and 15 μs .

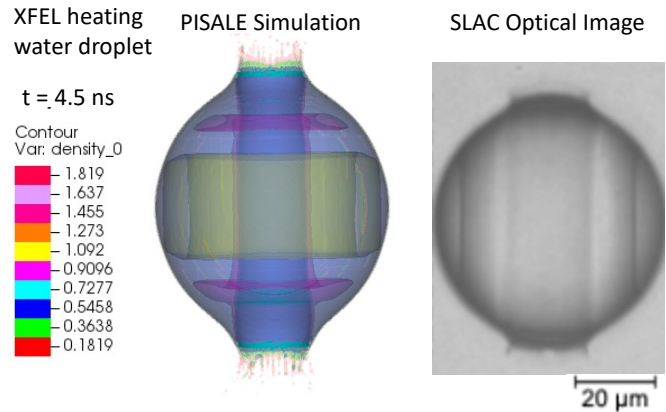


Fig. 6. Comparison of PISALE simulation of a water droplet heated by an XFEL with experimental image.

C. Modeling of SLAC experiments using XFEL beams

XFEL beams can be used to produce and study matter under extreme conditions. Liquids provide a means of bringing samples into the path of the X-ray beam for analysis. Ultrabright x-rays can blow up samples within a tiny fraction of a second, and modeling the dynamics of this interaction is critical to understanding which droplets can be used to collect data. These ultrashort ($\sim 50 fs$), high energy ($\sim 8 keV$), coherent x-ray sources can be used to both heat and probe targets. We discuss some recent results in modeling XFEL heating of water and hydrogen droplets. Figure 6 shows early time dynamics from a 3D PISALE simulation of a water droplet heated by an XFEL beam with a comparison to an experimental optical image [24] at the Coherent X-ray Imaging (CXI) instrument at SLAC. Previous work [19] modeling early stages of liquid-water-drop explosion showed 1D and 2D results assuming axisymmetry. This assumption is broken for later times due to distortions of the cavity boundary [19]. Therefore, the need of a 3D simulation not only as a diagnostic tool for early times,

but also for modeling reflection and spallation mechanisms that lead to fragmentation and expansion observed in water under extreme conditions at later times [25].

The need for High Repetition Rate (HRR) targets in High Energy Density Science has been stated many times as the areas moves towards HRR facilities [21] [13]. When using droplets as HRR targets, fratricide can occur. This is caused by the explosion of a heated droplet impacting the following droplet, which can make it ineffective for the following shot. The need to skip this perturbed droplet causes a reduction in the effective repetition rate and data acquisition quality. Figure 7 shows a 3D PISALE simulation of three hydrogen droplets with the first droplet (lowest in the image) already exploded after being heated by an XFEL beam. The image is 9 ns after the XFEL beam passes through the first droplet. The resulting explosion creates debris seen impacting the following droplets. The middle droplet is clearly perturbed by the debris causing a reduction of the effective repetition rate factor of this target system by at least by factor of 2 because this perturbed droplet cannot be used as a target. The XFEL beam travels along the x-axis, which passes through the center of the lowest droplet. The orientation (not the location) of the three axes is shown for the inline and side views.

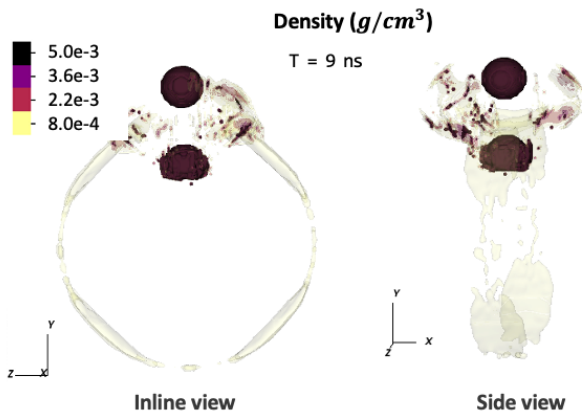


Fig. 7. Three dimensional PISALE simulation of three hydrogen droplets. The droplet following the XFEL heated droplet shields the second following droplet. The inline view is along the XFEL beam.

Surface tension can impact droplet dynamics in the lower temperature regions of this experiment. Early simulations show that enabling the surface tension package impacts the large-scale dynamics of the system. Figure 8 shows the side views of 3D PISALE simulations of hydrogen droplets with and without including surface tension effects. Even with surface tension forces included, the following droplet is still significantly perturbed by the exploding droplet. There is experimental evidence of larger water droplets heated by XFEL beams perturbing following droplets [24] but to our knowledge no published results for hydrogen droplets. Our modeling results for hydrogen show that fratricide is also a concern for these droplets and reduces the effective repetition rate.

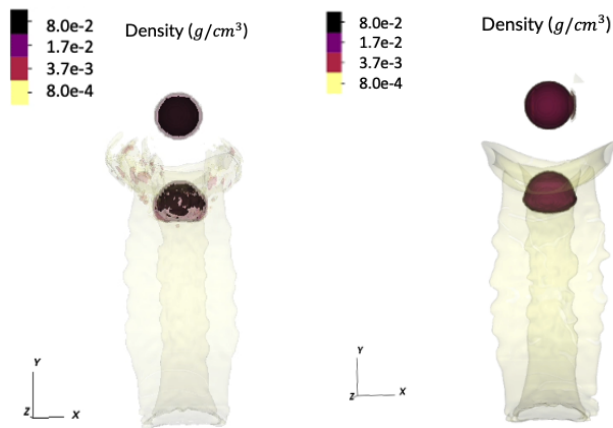


Fig. 8. Effects of surface tension are important for modeling. Comparison of PISALE simulation of hydrogen droplet heated by an XFEL without surface tension model (left) and including surface tension (right) at $t = 8$ ns.

IV. CONCLUSIONS AND FUTURE WORK

The PISALE code is being used in a wide variety of new areas showing excellent agreement with experimental data and contributing to a basic understanding of the physical processes. Three dimensional simulations are critical to most of these physical processes, and this is enabled through modern HPC platforms and appropriate numerical techniques and programming models. The combination of AMR with ALE is a powerful numerical approach with unique capabilities. Significant physics effects can be included in the numerical methods with careful implementation of the operator splitting approach. We are exploring paths discretize a wider array of PDEs relevant to plasma physics, mesoscale material modeling, seismicity in geophysics, and electromagnetics. We are also exploring a FEM framework with 3D AMR capability that would improve the existing heat conduction, radiation diffusion, and surface tension models in PISALE.

ACKNOWLEDGMENT

We would like to thank additional members of the PISALE team for their expertise and contribution to the code. The PISALE code is supported by the National Science Foundation, under Office of Advanced Cyber Infrastructure Award Number 2005259, the U.S. Department of Energy, Office of Science, under Fusion Energy Sciences Research Division Award Numbers DE-SC0021374 and DE-SC0023475, and the Office of Naval Research (ONR), under ONR MURI Award Number N00014-20-1-2682. This research used resources of the National Energy Research Scientific Computing Center (NERSC), a U.S. Department of Energy Office of Science User Facility located at Lawrence Berkeley National Laboratory, operated under Contract No. DE-AC02-05CH11231 using NERSC awards ERCAP0024761 and EERCAP0024762. The technical support and advanced computing resources from University of Hawaii Information Technology Services – Cyberinfrastructure, funded in part by the National Science

Foundation MRI award Number 1920304, are gratefully acknowledged.

REFERENCES

- [1] R. W. Anderson, N. S. Elliott, and R. B. Pember. "An arbitrary Lagrangian-Eulerian method with adaptive mesh refinement for the solution of the Euler equations". In: *Journal of Computational Physics* 199.2 (Sept. 2004), pp. 598–617.
- [2] J. Barnard et al. "NDCX-II target experiments and simulations". In: *Nuclear Instruments and Methods in Physics Research Section A: Accelerators, Spectrometers, Detectors and Associated Equipment* 733 (2014), pp. 45–50.
- [3] G. Bornia, A. Cervone, S. Manservigi, R. Scardovelli, and S. Zaleski. "On the properties and limitations of the height function method in two-dimensional Cartesian geometry". In: *Journal of Computational Physics* 230.4 (2011), pp. 851–862.
- [4] J. U. Brackbill, D. B. Kothe, and C. Zemach. "A continuum method for modeling surface tension". In: *J. Comput. Phys.* 100 (1992), pp. 335–354.
- [5] H.-J. G. Diersch. *FEFLOW: finite element modeling of flow, mass and heat transport in porous and fractured media*. Springer Science & Business Media, 2013.
- [6] D. C. Eder, A. C. Fisher, A. E. Koniges, and N. D. Masters. "Modelling debris and shrapnel generation in inertial confinement fusion experiments". In: *Nucl. Fusion* 53 (2013), p. 113037.
- [7] A. C. Fisher et al. "Modeling heat conduction and radiation transport with the diffusion Equation in NIF ALE-AMR". In: *Journal of Physics: Conference Series* 244 (2010), p. 022075.
- [8] B. T. N. Gunney and R. W. Anderson. "Advances in patch-based adaptive mesh refinement scalability". In: *Journal of Parallel and Distributed Computing* 89 (2016), pp. 65–84.
- [9] J. B. Habeck, M. D. Kroells, T. E. Schwartztruber, and G. V. Candler. "Characterization of particle-surface impacts on a sphere-cone at hypersonic flight conditions". In: *AIAA SCITECH 2023 Forum AIAA 2023-0205* (2023).
- [10] A. Koniges et al. "Multi-material ALE with AMR for modeling hot plasmas and cold fragmenting materials". In: *Plasma Sci. and Technol.* 17 (2015), pp. 117–128.
- [11] W. Liu et al. "Using a Korteweg-type model for modeling surface tension and its application". In: *54th Annual Meeting of the APS Division of Plasma Physics abstract id. BP8.058* (2012).
- [12] W. Liu et al. "Surface tension models for a multi-material ALE code with AMR". In: *Computers and Fluids* 151 (2017), pp. 91–101.
- [13] T. Ma et al. "Accelerating the rate of discovery: Toward high-repetition-rate HED science". In: *Plasma Physics and Controlled Fusion* 63.10 (2021), p. 104003.
- [14] N. D. Masters, T. B. Kaiser, R. W. Anderson, D. C. Eder, A. C. Fisher, and A. E. Koniges. "Laser ray tracing in a parallel arbitrary Lagrangian-Eulerian adaptive mesh refinement hydrocode". In: *Journal of Physics: Conference Series* 244 (2010), p. 032022.
- [15] J. McKee, Y. Mileyko, A. Fisher, and A. Koniges. "Developing a modern CFD framework with parallel algorithms and mesh adaptation". In: *Eleventh International Conference on Computational Fluid Dynamics (ICCFD11)* (2022). Paper 1301.
- [16] MFEM. <https://mfem.org/>. Accessed: 2023-09-18.
- [17] MOOSE. <https://mooseframework.inl.gov/>. Accessed: 2023-09-18.
- [18] C. Parisuana, D. C. Eder, M. Gauthier, C. Schoenwaelder, C. A. Stan, and S. H. Glenzer. "CFD modeling of droplets heated by an x-ray free electron laser". In: *Eleventh International Conference on Computational Fluid Dynamics (ICCFD11)* (2022). Paper 2003.
- [19] T. Paula, S. Adami, and N. A. Adams. "Analysis of the early stages of liquid-water-drop explosion by numerical simulation". In: *Physical Review Fluids* 4.4 (2019), p. 044003.
- [20] E. Pierazzo et al. "Validation of numerical codes for impact and explosion cratering: Impacts on strengthless and metal targets". In: *Meteoritics & Planetary Science* 43.12 (2008), pp. 1917–1938.
- [21] I. Prencipe et al. "Targets for high repetition rate laser facilities: needs, challenges and perspectives". In: *High Power Laser Science and Engineering* 5 (2017), e17.
- [22] M. A. Purvis et al. "Advancements in predictive plasma formation modeling". In: *Proc. SPIE 9776. Extreme Ultraviolet (EUV) Lithography VII*. 2016, 97760K–97760K.
- [23] Y. Seo, J. Lee, A. Koniges, and A. Fisher. "Development of the PISALE codebase for simulating flow and transport in large-scale coastal aquifer". In: *Eleventh International Conference on Computational Fluid Dynamics (ICCFD11)* (2022). Paper 1502.
- [24] C. A. Stan et al. "Liquid explosions induced by X-ray laser pulses". In: *Nature Physics* 12.10 (2016), pp. 966–971.
- [25] C. A. Stan et al. "Negative pressures and spallation in water drops subjected to nanosecond shock waves". In: *The journal of physical chemistry letters* 7.11 (2016), pp. 2055–2062.
- [26] M. L. Wilkins. *Computer simulation of dynamic phenomena*. Springer Science & Business Media, 1999.
- [27] P. T. Yip et al. "Arbitrary Lagrangian Eulerian simulations of high speed particle impacts encountered during hypersonic flight". In: *Eleventh International Conference on Computational Fluid Dynamics (ICCFD11)* (2022). Paper 2202.